Available online at www.sciencedirect.com
SCIENCE DIRECT®
International Journal of Heat and Mass Transfer 49 (2006) 3626–3633
International Journal of HEAT and MASS TRANSFER
www.elsevier.com/locate/ijhmt

Numerical analysis of the dynamics of moving vapor bubbles

David M. Christopher *, Hao Wang, Xiaofeng Peng

Department of Thermal Engineering, Tsinghua University, Beijing 100084, China

Received 3 December 2004; received in revised form 1 December 2005
Available online 18 April 2006

Abstract

Bubbles have been observed rapidly sweeping along very fine heated wires during subcooled nucleate boiling with jet flows emanating from the tops of the vapor bubbles. This paper analyzes the physical mechanisms driving the bubble and the jet flows from the tops of these moving bubbles. The flows are analyzed by numerically solving the governing equations for the velocity and temperature distributions around the bubble and the heated wire as the bubble moves along the wire. The bubble motion is due to the non-uniform temperature distribution in the liquid and in the wire caused by the bubble as it moves along the wire. The flow is driven by the horizontal Marangoni flow induced by the temperature difference across the bubble which thrusts the bubble forward. Comparisons with experimental observations suggest that the condensation heat transfer at the bubble interface is restricted by non-condensable gases that increases the surface temperature gradient and the resulting Marangoni flow.

Keywords: Nucleate boiling; Bubble motion; Marangoni flow; Evaporation

1. Introduction

Nucleate boiling is encountered in many fields, such as energy utilization, manufacturing processes and chemical processing. In the last part of the 20th century, boiling has been increasingly applied to many new areas, such as spacecraft thermal control, electronic cooling, and bioengineering. However, even though a wide variety of boiling models exist, no general theoretical models accurately predict boiling heat and mass transfer rates over a variety of conditions and even the basic mechanisms are not entirely understood [1,2]. Dhir [1] presented an extensive review of the available research, but noted that "Boiling is an extremely complex and illusive process, which continues to baffle and challenge inquisitive minds."

The phenomena of bubble motion along a heated wall has been investigated many times, especially in forced flow boiling, tube boiling and boiling on downward facing or inclined walls. During forced convection boiling on vertical walls with upflow [3], the bubbles slide along the heater wall and typically do not lift off, while with downflow, the bubbles either lift off directly from the nucleation site or slide some and then lift off. The process of vapor bubble sliding appears to enhance the energy transfer from the heating surface as evidenced by larger heat transfer coefficients for upflow than for downflow under otherwise identical operating conditions. Similarly, heat transfer with boiling around tubes is more due to bubbles sliding around the tubes than the nucleation on the surface [4–6]. Cornwell et al. [5] and Cornwell and Grant [6] analyzed the contribution of bubble motion to the heat transfer to show that heat transfer was largely through a thin layer of liquid under the bubble as the bubble slid.

At the microscale level, the flows in and around a vapor bubble attached to a wall during nucleate boiling form the basis for the boiling heat transfer mechanisms. Larkin [7] gave perhaps the first reported observation of thermocapillary jet flows (Marangoni convection) emanating from the tops of vapor bubbles. The development of digital measurement and visualization techniques has provided a new tool for studying these microscale heat transfer mechanisms during boiling. Peng et al. [8] observed

* Corresponding author. Tel.: +86 10 6277 2986; fax: +86 10 6277 0209.
E-mail address: dmc@tsinghua.edu.cn (D.M. Christopher).

0017-9310/$ - see front matter © 2006 Elsevier Ltd. All rights reserved.
doi:10.1016/j.ijheatmasstransfer.2006.02.039

Nomenclature

A_b	bubble surface area
A_w	wire cross-sectional area
c	specific heat
F_P	pressure force on bubble
F_{thrust}	thrust acting on the bubble
h	convection coefficient
h_{fg}	heat of vaporization
h_j	equivalent interfacial heat transfer coefficient
k	z-direction unit vector
$\overline{M}$	vapor molecular weight
n	normal direction
$\overline{R}$	universal gas constant
p	pressure
P_w	wire perimeter
Q	distributed energy source term in wire
Q_b	localized energy source term in wire due to bubble
R_b	bubble radius
s	tangential direction
t	time
T	temperature
T_v	vapor temperature
$\hat{T}$	excess temperature in wire
u, v	velocities
U	bubble velocity
x, y, z	Cartesian coordinates

Greek symbols

α	thermal diffusivity
ϕ	polar angle from the z-axis
λ	wire thermal conductivity
μ	dynamic viscosity
ρ_v	vapor density
θ	azimuthal angle in the x–y plane from the x-axis, temperature difference
σ	surface tension
$\hat{\sigma}$	accommodation coefficient
$\tau_{r,\phi}$	tangential shear stress
ξ	moving z-coordinate

Subscripts

1	convection coefficient before bubble
2	convection coefficient after bubble
b	back side of bubble
f	front side of bubble
s	bubble surface, saturation
w	wire
v	vapor; vertical
x, y, z	coordinate directions
∞	ambient conditions
r, θ, ϕ	spherical coordinate directions

nucleation jets from inverted stationary vapor bubbles. Wang et al. [9–12] observed various types of jet flows emanating from nucleation sites on microwires and from bubbles on the microwires including stationary bubbles and bubbles sweeping along the microwires with jet plumes trailing behind the bubbles. Single and multiple jet flows were observed around both stationary and moving bubbles [13] with numerical investigations showing that for stationary bubbles, multiple jets would develop if the bubble diameter was larger than the wire diameter. Bubble sweeping on ultrathin wires was observed for a variety of conditions with bubble sweeping observed on horizontal, vertical and inclined wires with the observed sweeping velocities seemingly independent of the orientation [14]. Wang et al. [14] also observed bubble motion on the sides of the heated wires as well as the tops. For stationary vapor bubbles, Wang et al. [15] observed that the measured velocities in the bubble top jets were essentially independent of orientation relative to gravity indicating that buoyancy was not the primary mechanism driving the flows. Bubbles have also been observed returning towards the wire after some perturbation pushed the bubble away from the wire (usually another smaller bubble) with calculations showing that the thrust from the Marangoni flow is sufficient to cause the bubble to return [16].

Analysis of the flow dynamics of stationary bubbles on microwires [13] showed that Marangoni flow is the most significant force driving the flows around the vapor bubbles. Their experimental and numerical results both verified that natural convection had little effect on the flow field, most likely due to the very small size of the wires. The flow dynamics around a bubble on a flat surface, either above or below the heated surface, would be very different due to the much larger area of the heated surface.

The present paper presents a natural extension of the analysis of flows around stationary bubbles [13] to the much more complex analysis of the fluid and thermal dynamics driving the bubble motion observed along heated ultrathin platinum wires and the thermal jets observed flowing from the tops of these bubbles. The analysis is based on the experimental conditions for ethanol, but similar moving bubbles were also observed in water. The analysis considers the effects of natural convection and Marangoni flow as well as the heat transfer due to the convection and evaporation within the bubble.

2. Theoretical analysis

2.1. Bubble sweeping dynamics

Vapor bubbles have been observed moving along heated wires due to Marangoni flow from the front to the rear of the bubble driven by the surface tension gradient occurring

when the front bubble surface is warmer than the rear surface. Marangoni flow occurs because the surface tension for nearly all fluids decreases with temperature so that fluid is pulled from higher temperature regions to lower temperature regions along the liquid surface. The bubble depresses the wire and fluid temperatures in the vicinity of the bubble due to the larger heat transfer caused by the bubble as compared to natural convection [10]. As the bubble then begins to move due to some perturbation, the leading edge of the bubble moves into warmer fluid while the trailing edge is exposed to cooler fluid. Thus, the front surface will be warmer than the back surface creating Marangoni flow from the front to the back which provides thrust to further move the bubble forward. The bubble quickly accelerates until the increasing drag balances the thrust. The motion continues until the bubble encounters some obstacle, typically another bubble. A numerical analysis was, therefore, used to verify if the Marangoni thrust was sufficient to drive the bubbles at the observed velocities of 20–60 mm/s.

Marangoni flow also occurs in the vertical direction from the bottom to the top of the bubble due to the vertical temperature gradient along the bubble interface. Since the vertical temperature gradient is much larger than the horizontal temperature gradient, the vertical velocities are larger with obvious jet plumes observed in the experiments. The jet plumes were especially evident in the jet plumes above stationary bubbles [15] but were also observed emanating from moving bubbles. The experimental observations also showed that the bubbles moved up and down along vertical wires and along inclined wires, indicating that the dynamics are independent of gravity. The velocities of the jet flows from the bubble tops were also essentially independent of the orientation to gravity, so this description of the dynamics refers to a bubble on a horizontal wire only to simplify the description. The most significant observation of the effects of gravity is that no bubbles were observed moving along the underside of wires even though stationary bubbles with downward flowing bubble top jets were observed underneath the wires. While buoyancy would be expected to cause moving bubbles to slide around to the top of the bubble, the results also show that the thinner natural convection boundary layer underneath the wire also severely limits the bubble motion due to the smaller induced temperature gradients along the bubble interface.

2.2. Numerical solution of the Navier–Stokes equations

A typical moving bubble is shown in Fig. 1. The measured bubble movement velocities were typically in the range of 20–60 mm/s with the bubbles very quickly accelerating to a steady-state speed. Therefore, the analysis only considers the steady-state bubble dynamics since the bubble velocities were constant most of the time. The three-dimensional flow geometry shown in Fig. 2 included the heated wire, the bubble with evaporation and condensation

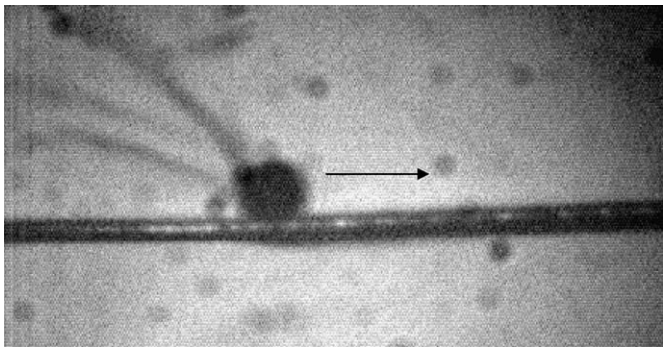

Fig. 1. Typical moving bubble with trailing jets.

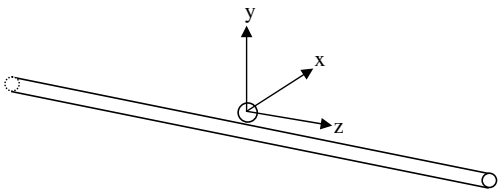

Fig. 2. Bubble-jet geometry and coordinate system with the bubble moving in the z-direction.

at its surface and a large liquid region around the bubble. The bottom surface of the bubble was assumed to be separated from the wire surface by a 2 μm thick microlayer based on visual observations made during the experiments that the bubbles did not seem to be actually touching the wire and on Sharp's [17] observations that the microlayer is 0.5–2.5 μm thick. Simulations of stationary bubbles with 1.5 μm or 2 μm thick microlayers yielded essentially the same flow velocities and heat transfer rates [13] so the uncertainties in the microlayer thickness are thought to not have a significant effect on the overall results. The bubble is held to the wire not by surface tension forces since the contact area is very small, but by the thrust of the vertical Marangoni flow from the bubble top. The flow and heat transfer were analyzed by numerically solving the steady-state, laminar, three-dimensional Navier–Stokes equations with the energy equation [13]. The problem statement was transformed so that the bubble was stationary while everything else moved at the experimentally observed bubble velocity in a moving Cartesian coordinate system, including the wire and the outer surface of the computational domain.

The energy equation boundary conditions included a heat source in the wire, Q, and a specified bulk subcooling temperature at the outer boundary which was about 30 bubble diameters away from the wire. The outer boundary was specified as a moving, solid wall to facilitate convergence. Tests with larger boundaries and open (constant pressure) boundaries indicated that the outer boundary was sufficiently far removed to have no effect on the flow field near the bubble. The boundary condition at the bubble interface used to model the evaporation and

condensation at the interface was based on a convective heat transfer coefficient [15]

$$h_j = \frac{2\hat{\sigma}}{2-\hat{\sigma}} \frac{h_{fg}^2 \rho_v}{T_v} \left(\frac{\bar{M}}{2\pi \bar{R} T_v}\right)^{1/2} \left[1 - \frac{p_v}{2h_{fg}\rho_v}\right] \quad (1)$$

and a vapor temperature equal to the saturation temperature for the pressure inside a bubble of the given size based on the LaPlace and Clausius–Clapeyron equations:

$$T_v = T_s + \frac{2\sigma T_s}{h_{fg}\rho_v R_b} \quad (2)$$

For ethanol at atmospheric pressure with the bubble radius of 0.1 mm used in most of the calculations, the correction to the vapor temperature in Eq. (2) is only about 0.1 °C. The accommodation coefficient in Eq. (1) is generally assumed to be 0.03 as suggested for water [15].

The momentum equation boundary conditions at the wire were the no slip condition with the wire moving at the bubble velocity. The boundary condition for the momentum equation at the bubble interface was modeled using the Marangoni boundary condition:

$$-\mu\left(\frac{\partial u_s}{\partial n}\right)_{R_b} = \frac{\partial \sigma}{\partial T}\left(\frac{\partial T}{\partial s}\right)_{R_b} \quad (3)$$

where n indicates the normal direction and s indicates the tangential direction to the interface.

The inlet conditions were a specified uniform axial flow velocity equal to the bubble velocity with the u, v and T distributions calculated assuming pure natural convection from the wire as would occur for an undisturbed wire in the liquid pool.

The equations were solved using the finite volume method with second-order central differencing of the advection terms using FLUENT 6.0. First-order upwind differencing was first used to approach a converged solution with the differencing method then changed to second-order central differencing to finish the calculation. A large jump in the wire temperatures was typically observed when the differencing method was changed. The QUICK method [18] gave the same results as the second-order central differencing.

The grid included about 320,000 tetrahedral elements with a double layer of hexahedrons on the bubble interface since the Marangoni boundary condition calculation is most accurate with hexahedrons. Calculations with about 450,000 elements yielded similar results, in terms of the bubble velocity, fluid velocities and heat fluxes, to those described here. The results with about 120,000 elements were somewhat different with lower equilibrium bubble velocities and an unrealistic temperature distribution along the wire due to the restricted heat transfer between the bubble and the wire caused by the small number of elements there.

2.3. Equilibrium force balance on the bubble

The bubble velocity (actually the velocities of the inlet, the wire and the outer surface) was based on the equilibrium between the pressure drag on the bubble and the horizontal thrust caused by the Marangoni flow. The pressure drag on the bubble was calculated by integrating the pressure component in the z-direction over the bubble surface.

$$F_P = \int p(\vec{n}\cdot k)\mathrm{d}A_b \quad (4)$$

The thrust due to the Marangoni flow along the bubble interface was calculated by integrating the z component of the tangential shear stress, $\tau_{r,\phi}$, over the bubble surface.

$$F_{thrust} = \int (-\tau_{r,\phi} sin(\phi))\mathrm{d}A_b \quad (5)$$

A negative value indicates thrust while a positive value indicates drag. The bubble will move at uniform velocity when the pressure force on the bubble given by Eq. (4) and the thrust on the bubble given by Eq. (5) are balanced.

2.4. Analytical solution for the wire temperature

The heat transfer from the bubble to the wire can be approximated as a moving point source in a wire with uniform heat generation and convection from the outside of the wire. However, the convection from the wire before the bubble passes is only due to natural convection while the convection after the bubble passes is due to significantly more fluid motion due to the bubble wake; therefore, the heat transfer coefficient around the wire is higher behind the bubble than in front of it. The governing equation for the temperature distribution in the wire is the one-dimensional, transient heat conduction equation with the convection heat flux from the surface treated as a heat loss term

$$\rho c \frac{\partial T}{\partial t} = \lambda \frac{\partial^2 T}{\partial z^2} - \frac{hP_w(T - T_\infty)}{A_w} + Q \quad (6)$$

where the convection coefficient before the wire is h_1 and that after the wire is h_2. The solution was adapted from the moving heat source solutions given by Eckert and Drake [19]. After transforming the time derivative to a moving z derivative and defining the temperature difference θ as $T - T_\infty$, Eq. (6) becomes

$$\frac{\partial^2 \theta}{\partial \xi^2} + \frac{U}{\alpha}\frac{\partial \theta}{\partial \xi} - \frac{hP_w}{\lambda A_w}\theta + \frac{Q}{\lambda} = 0 \quad (7)$$

where $h = h_1$ for $\xi < 0$ and $h = h_2$ for $\xi > 0$ and $\xi = z - U * t$ with U as the moving source velocity (i.e., the bubble velocity). The boundary conditions are that the temperatures at $z = \pm\infty$ are equal to the excess heat temperatures due to the heat generation defined as

$$\hat{T}_{z=-\infty} = \frac{QA_w}{h_1 P_w} + T_\infty, \quad \hat{T}_{z=+\infty} = \frac{QA_w}{h_2 P_w} + T_\infty \quad (8)$$

and that the sum of the heat transfer rates at $z = 0$ from both directions is equal to the heat transfer due to the moving source which in this case is the bubble heat transfer, Q_b.

The interface temperature between the solutions for ξ less than zero and for ξ greater than zero is

$$T(\xi=0)-T_\infty = \frac{\frac{Q_b}{\lambda A_w}+\frac{QA_w}{h_1P_w}\left(\sqrt{\left(\frac{U}{2\alpha}\right)^2+\frac{h_1P_w}{\lambda A_w}}-\frac{U}{2\alpha}\right)+\frac{QA_w}{h_2P_w}\left(\sqrt{\left(\frac{U}{2\alpha}\right)^2+\frac{h_2P_w}{\lambda A_w}}+\frac{U}{2\alpha}\right)}{\sqrt{\left(\frac{U}{2\alpha}\right)^2+\frac{h_1P_w}{\lambda A_w}}+\sqrt{\left(\frac{U}{2\alpha}\right)^2+\frac{h_2P_w}{\lambda A_w}}} \quad (9)$$

The solution for $\xi<0$ is then:

$$T(\xi)=\left(T_0-\frac{\dot{Q}A_w}{h_1P_w}-T_\infty\right)e^{\left(\sqrt{\left(\frac{U}{2\alpha}\right)^2+\frac{h_1P_w}{\lambda A_w}}-\frac{U}{2\alpha}\right)\xi}+\frac{\dot{Q}A_w}{h_1P_w}+T_\infty \quad (10)$$

while the solution for $\xi>0$ is:

$$T(\xi)=\left(T_0-\frac{\dot{Q}A_w}{h_2P_w}-T_\infty\right)e^{-\left(\sqrt{\left(\frac{U}{2\alpha}\right)^2+\frac{h_2P_w}{\lambda A_w}}+\frac{U}{2\alpha}\right)\xi}+\frac{\dot{Q}A_w}{h_2P_w}+T_\infty \quad (11)$$

As will be shown in the results, these two equations give a reasonable approximation of the wire temperature distribution given by the numerical solution of the 3D Navier–Stokes equations for the entire flow field.

3. Results

The experimentally observed movement of vapor bubbles along heated wires was analyzed by solving the Navier–Stokes and energy equations to model the flow around the bubble moving along a heated wire. The results reported here are based on the properties of ethanol at the boiling point, 77 °C. Similar results were observed in water. The two bubble sizes analyzed in the calculations had diameters of 0.2 mm and 0.4 mm, which were typical of the experimentally observed bubbles. The wire was made of platinum with a diameter of 0.1 mm. The bulk liquid subcooling was varied from 20 °C to 50 °C as in the experiments. For these conditions, the convective heat transfer coefficient at the bubble interface given by Eq. (1) was 153 000 W/m^{2}K. Since these bubbles were relatively large, the saturation temperature at the vapor pressure inside the bubble would also be essentially 77 °C. The wire temperatures in the experiments were 10 °C–15 °C above saturation with heat generation rates in the wire of about 1×10^{10} W/m^3 with several percent of the energy lost from the wire to the supports. In the analysis, the heat generation rates in the wire were adjusted until the evaporation and condensation rates in the bubble were in equilibrium, which resulted in heat generation rates that were 10–20% less than the experimental values. The predicted wire superheats and bubble velocities agreed well with the measured values.

3.1. Numerical results

The numerical solution of the governing equations for the 3D velocity and temperature distributions yielded average wire temperatures for the various cases which were all within the experimental uncertainties of the measured temperatures. For the calculations, the bubble velocity was varied until the pressure drag and the thrust were in equilibrium, which would indicate a steady-state velocity. The analysis showed that for these conditions, the bubble heat transfer rate could only be balanced if the condensation heat transfer coefficient within the bubble was much less than the evaporation rate. Marek and Straub [20] showed that the condensation heat transfer coefficient could be reduced by more than 90% by a very small amount of non-condensable gases. The evaporation coefficient is probably not affected by the non-condensable gases, or the effect is quite small, because such gases tend to accumulate at the condensing surface. A reduced condensation rate increases the Marangoni flow driving force because it increases the temperature gradient along the bubble interface. The calculations showed that for these conditions, the thrust could only balance the pressure drag if the condensation heat transfer coefficients were at least 20 times smaller than the evaporation coefficients.

A typical temperature distribution along the centerplane passing though the center of the bubble and the center of the wire is shown in Fig. 3. These results are for a bubble moving to the left with a velocity of 28.3 mm/s, a diameter of 0.2 mm, a subcooling of 30 °C, a heat generation rate of 3.6×10^9 W/m^3, an average wire temperature of 81.9 °C and an evaporation/condensation heat transfer coefficient ratio of 100. The microlayer between the bubble and the wire is not visible in Fig. 3 since it is less than the line thickness. The thermal hydraulics were analyzed for various bubble velocities until the horizontal component of the thrust generated by the Marangoni flow balanced the horizontal force due by the pressure distribution as described in Section 2.3. The calculation was based on the properties of ethanol at its boiling point. The plume observed in the

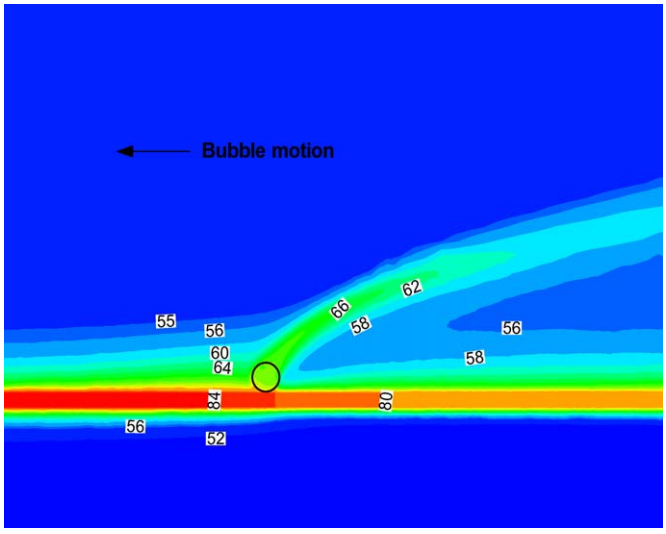

Fig. 3. Temperature distribution around a vapor bubble moving along a heated wire at 28.3 mm/s.

experiments is evident in the temperature distribution. Such a distinctive plume can only occur as a result of Marangoni flow along the interface. The calculated velocities near the bubble ranged from 50–100 mm/s which agrees with the range of velocities measured using a PIV system for these conditions [15]. The temperature contours on the bubble interface are shown in Fig. 4 for the same conditions. Two low temperature regions formed on the top and on the upper part of the back side. The Marangoni effect causes the liquid on the surface to flow towards these two minimum temperature locations with jets leaving the surface at these points. However, these jets quickly coalesce into one jet above the bubble for these flow conditions. The surface velocities are largest at the bottom where the temperature gradient is the largest and decrease upward along the interface. The surface velocities are the lowest between the two low temperature regions with a small recirculating zone above the bubble between these two points which reduces the heat transfer in that area and increases the surface temperature.

Fig. 3 also shows that the moving bubble absorbs the energy in the boundary layer around the wire as it moves across the wire. The liquid temperature distribution in front of the bubble shows a normal heated boundary layer around the wire. However, the temperature distribution behind the bubble shows that the liquid in what was the boundary layer region is substantially cooler due to the heat transfer to the bubble. The temperature difference in the liquid regions just in front of and just behind the bubble then contribute to the surface temperature differences on the bubble. The reduced heat transfer due to the higher fluid temperatures in the front would be somewhat increased by the higher heat transfer coefficients caused by the flow impinging the front of the bubble; however, since the front surface of the bubble is hotter than the back surface, the effect of the different fluid temperatures on the heat transfer is more important than the effect of the different heat transfer coefficients.

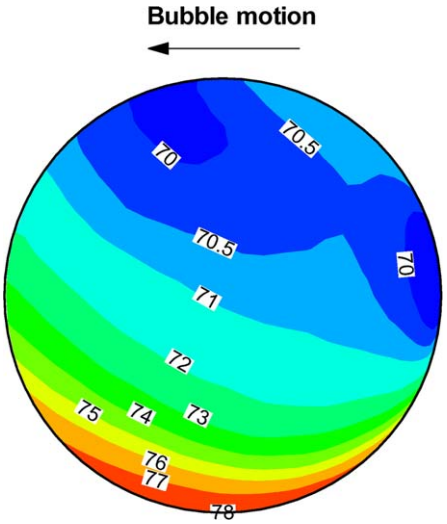

Fig. 4. Temperature contours on bubble surface. The dark blue spots are the coolest while the orange region at the bottom is the hottest. (For interpretation of the references to colour in this figure legend, the reader is referred to the web version of this article.)

Other numerical results not presented here clearly showed that natural convection without Marangoni flow could not create such a distinctive plume and resulted in maximum velocities that were far less than measured experimentally.

The numerical results verify that Marangoni flow is the most likely mechanism causing the bubble to move. The thrust in Eq. (5) pushing the bubble forward is the result of the horizontal component of the velocities along the bubble interface, which is the result of the horizontal temperature gradient along the bubble interface. The surface temperatures shown in Fig. 4 decrease from the front towards the back (left to right in Fig. 4) with a temperature difference from the front to the back of the bubble of about 2 °C. Although most of the flow is directed upwards, the flow has a small horizontal component that is sufficient to push the bubble forward. The temperature gradient from the front to the back occurs as the large amount of heat transfer associated with the bubble cools the liquid and the wire near the bubble causing the liquid behind the bubble and the back side of the bubble to be cooler than the front side.

The surface normal velocities due to the evaporation and condensation at the bubble interface can also be estimated from the numerical results. The maximum evaporation rate, which occurred only in a very small region near the wire, was approximately 6×10^5 W/m^2 which would result in a liquid velocity normal to the bubble interface of less than 1 mm/s which is far less than the velocities in that region. The condensation rates were far less since they were spread over a much larger area, so the velocities due to condensation would also be negligible. Although the surface normal velocities due to evaporation and condensation can be neglected, the heat transfer due to evaporation and condensation can not be neglected since both significantly affect the temperature distribution around the bubble. In addition, further calculations showed that if the evaporation and condensation heat transfer are neglected, the top of the bubble is much cooler than the bottom resulting in extremely large, unrealistic velocities due to the Marangoni flow. Therefore, the heat transfer effects were included in the numerical model while the resulting normal velocities were not.

The heat flux from the wire surface behind the bubble was significantly increased by the Marangoni flow around the bubble and by the flow disturbances due to the wake behind the bubble. Although the maximum heat flux occurred directly underneath the bubble, the area affected by the wake behind the bubble was much larger which resulted in more heat transfer from this area than from underneath the bubble. The heat transfer in this wake region was enhanced by relatively cool fluid drawn up from below the wire by the Marangoni effect and by the disrupted boundary layer which substantially increase the

cooling of the wire in that area. Typical heat transfer rates in the wake region were 3–6 times greater than the heat transfer due to evaporation from the liquid region directly underneath the bubble.

3.2. Analytical results using the model in Section 2.4

The predicted wire temperature distribution given by the analytical solution described in Section 2.4 is compared with the wire temperatures given by the numerical solution for the entire flow field in Fig. 5. The moving heat source that represents the excess heat transfer due to the bubble and the Marangoni flow around the bubble, $Q = 0.0027$ W is at $\xi = 0$. The heat transfer coefficients before and after the bubble were calculated using the average heat flux on the wire and the average wire temperatures given by the numerical solution 1 mm before the bubble and 2 mm after the bubble. Fig. 5 shows that the analytical solution given by Eqs. (10) and (11) gives a reasonable representation of the full numerical solution so Eqs. (10) and (11) can be used to model the heat transfer in the wire as the bubble passes by. This result also confirms that the relatively large heat transfer rate due to Marangoni induced flow around the wire in the bubble wake must be included in the heat transfer model. The relatively lower surface temperatures after the bubble passes explain the significantly lower nucleation rates observed experimentally for some time after the bubble passes until the wire surface temperature again recovers back to its original value. The relative temperatures before and after the bubble are very sensitive to the heat transfer coefficients before and after the bubble. For example, if the heat transfer coefficient behind the bubble were the same as in front of the bubble, the temperature behind the bubble would increase rather than decrease very soon after the bubble passes. The temperature at $\xi = 0$ predicted by the analytical model for unequal heat transfer coefficients, Eq. (9), was 82.2 °C, which was the same as that predicted by the numerical model. The temperature difference between the locations on the wire corresponding to the front and rear surfaces of the bubble was 0.9 °C for the conditions in Fig. 5. The temperature difference from the front to the back of the bubble calculated from the data in Fig. 4 was 2 °C which again indicates the importance of the heated boundary layer fluid impinging the front of the bubble on the heat transfer to the bubble interface.

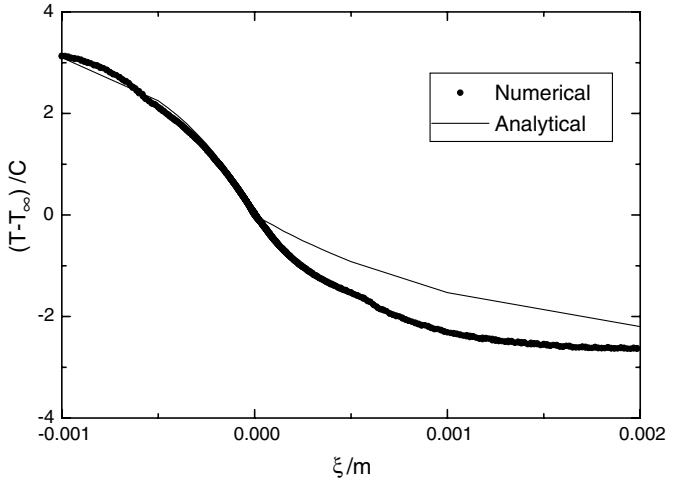

Fig. 5. Temperature distribution along the wire for ethanol with a subcooling of 30 °C, a bubble diameter of 0.2 mm, a bubble velocity of 28.3 mm/s, and a heat generation rate of 3.6×10^9 W/m^3.

3.3. Effects of flow conditions on the bubble movement

Variations in the evaporation and condensation heat transfer coefficients (which are essentially proportional to the accommodation coefficients) significantly affected the heat transfer rates and bubble velocities. Equal evaporation and condensation accommodation coefficients (increased condensation heat transfer coefficient compared to the results in Figs. 3 and 4) resulted in no bubble motion because the much reduced temperature differences in the horizontal and vertical directions resulted in very little Marangoni flow around the bubble. The lack of motion then actually reduced the heat transfer from the wire. Significantly reduced condensation heat transfer coefficients (with the evaporation coefficient kept constant) resulted in slightly less heat transfer but larger bubble velocities as the larger temperature differences across the bubble created more horizontal Marangoni flow and thus more thrust.

Increases in the liquid subcooling increased the bubble velocity and the heat transfer from the wire since the cooler bulk liquid temperature not only increases the heat transfer from the bubble and the wire to the liquid but also the temperature difference across the bubble which increases the bubble velocity. The effect of liquid subcooling was also observed experimentally with large subcoolings required to generate the observed bubble motions.

Analysis of the flow and temperature fields around a larger 0.4 mm diameter bubble showed that the larger bubble increases the heat transfer from the wire by about 20% while reducing the bubble velocities by about 30%. The bubbles velocities are lower because the larger bubble creates more drag and since even though the larger bubble has a larger temperature difference across the bubble surface, the temperature gradient is less which reduces the Marangoni flow.

Experimental observations have shown that the bubble top jet flows are essentially independent of orientation relative to gravity with bubble top jet flows going sideways and down as well as up. Bubble motion was also observed on vertical wires with bubbles moving both up and down the wire at essentially the same velocities; however, bubbles were not observed moving underneath the heated wires. The numerical results confirmed that bubble motion under the wire is less likely with a much lower bubble velocity of 8.0 mm/s predicted for the 0.2 mm diameter bubble with a subcooling of 30 °C (rather than 28.3 mm/s for a bubble on top of the wire). The bubble moves much slower because the heated boundary layer under the wire is much smaller

than on top of the wire so that as the bubble moves along the wire, the temperatures around the bubble are more uniform which reduces the Marangoni flow driving the bubble. Even though the bubble velocity was reduced, the heat transfer due to a bubble underneath the wire was increased by about 30% relative to the case with a bubble on top of the wire. Of course, buoyancy would also tend to push a moving bubble from underneath the wire to on top of the wire.

4. Conclusions

The heat transfer and fluid motion around a nucleation bubble moving on a heated wire were analyzed numerically by solving the Navier–Stokes equations with the energy equation. The results show that the bubble motion must be driven by Marangoni flow due to the temperature difference between the front and the back surfaces of the bubble. The evaporation and condensation velocities normal to the interface were too small too significantly influence the velocity field; although the heat transfer due to the evaporation and condensation is very significant. The results also show that the temperature gradients on the bubble surface and the resulting Marangoni flow will not be strong enough to move the bubble unless non-condensable gases or some other mechanism is present to reduce the condensation heat transfer at the interface. The calculations show that reductions in the condensation heat transfer while reducing the overall heat transfer, work to increase the bubble velocity.

The numerical results show that the convection heat transfer due to the Marangoni driven flow along the wire surface is significantly greater than the heat transfer directly attributable to the evaporation under the bubble. The results also show that, as expected, larger liquid subcoolings result in increased heat transfer rates and increased bubble velocities.

A simple analytical solution for the temperature distribution in the wire given as a function of the heat transfer due to the bubble was shown to reasonably represent the wire temperature to give further insight into the mechanisms driving the bubble motion.

Acknowledgements

This project was supported by the National Natural Science Foundation of China (Contract No. 50476014).

References

[1] V.K. Dhir, Nucleate and transition boiling heat transfer under pool boiling and external flow conditions. In: Proc. of the Ninth Int. Heat Transfer Conf., Hemisphere, New York, 1990, vol. 1, pp. 129–155.
[2] V.P. Carey, Liquid vapor phase-transition phenomena, Hemisphere, New York, 1992.
[3] G.E. Thorncroft, J.F. Klausner, R. Mei, An experimental investigation of bubble growth and detachment in vertical upflow and downflow boiling, Int. J. Heat Mass Transfer 41 (23) (1998) 3857–3871.
[4] Cornwell K., The role of sliding bubble in boiling on tube bundles. In: Proc. of the Ninth Int. Heat Transfer Conf., Jerusalem, Israel, Hemisphere, New York, 1990, pp. 455–460.
[5] K. Cornwell, S.D. Houston, A.J. Addlesee, Sliding bubble heat transfer on a tube under heating and cooling conditions, in: Pool and External Flow Boiling, Eng. Foundation Conf., ASME, Santa Barbara, NY, 1992, pp. 49–53.
[6] K. Cornwell, I.A. Grant, Heat transfer to bubbles under horizontal tubes, Int. J. Heat Mass Transfer 41 (10) (1998) 1189–1197.
[7] B.K. Larkin, Thermocapillary flow around hemispherical bubbles, AICHE J. 16 (1) (1970) 101–107.
[8] X.F. Peng, Y.J. Huang, D.J. Lee, Transport phenomenon of a vapor bubble attached to a downward surface, Int. J. Therm. Sci. 40 (9) (2001) 797–803.
[9] H. Wang, X.F. Peng, B.X. Wang, D.J. Lee, Jet Flow Phenomena during Nucleate Boiling, Int. J. Heat Mass Transfer 45 (6) (2002) 1359–1363.
[10] H. Wang, X.F. Peng, B.X. Wang, D.J. Lee, Bubble sweeping mechanisms, Sci. China Ser. E 46 (3) (2003) 223–225.
[11] H. Wang, Multiplicity of Nucleation and Near-wall Bubble Dynamics of Subcooled Boiling on Micro Wires. Ph.D. thesis, Tsinghua University, Beijing, 2004.
[12] H. Wang, X.F. Peng, B.X. Wang, D.J. Lee, Bubble Sweeping and Jet Flows during Nucleate Boiling of Subcooled Liquids, Int. J. Heat Mass Transfer 46 (5) (2003) 863–869.
[13] H. Wang, X.F. Peng, D.M. Christopher, W.K. Lin, C. Pan, Investigation of bubble-top jet flow during subcooled boiling on wires, Int. J. Heat Fluid Flow 26 (3) (2005) 485–494.
[14] H. Wang, X.F. Peng, B.X. Wang, W.K. Lin, C. Pan, Experimental observations of bubble dynamics on ultrathin wires, Exp. Heat Transfer 18 (1) (2005) 1–11.
[15] H. Wang, X.F. Peng, W.K. Lin, C. Pan, B.X. Wang, Bubble-top jet flows on microwires, Int. J. Heat Mass Transfer 47 (2004) 2891–2900.
[16] H. Wang, X.F. Peng, S.V. Garimella, D.M. Christopher, Microbubble Return Phenomena during Subcooled Boiling on Small Wires, Int. J. Heat Mass Transfer, submitted for publication.
[17] Sharp, R.R., The Nature of Liquid Film Evaporation during Nucleate Boiling, October, 1964, NASA TND-1997.
[18] B.P. Leonard, A stable and accurate convective modeling procedure based on quadratic upstream interpolation, Comput. Meth. Appl. Mech. Eng. 19 (1979) 59–98.
[19] E.R.G. Eckert, R.M. Drake, Analysis of Heat and Mass Transfer, McGraw-Hill, New York, 1972.
[20] R. Marek, J. Straub, The Origin of Thermocapillary Convection in Subcooled Nucleate Pool Boiling, Int. J. Heat Mass Transfer 44 (3) (2001) 619–632.